Journal of Alloys and Compounds 509 (2011) 7677–7683

Contents lists available at ScienceDirect

Journal of Alloys and Compounds

journal homepage: www.elsevier.com/locate/jallcom

Calculation of band offsets in $Cd_{1-x}X_xTe$ alloys, X = Zn, Mg, Hg and Mn and magnetic effects in CdMnTe

S. Abdi-Ben Nasrallah [a,*], S. Mnasri [a], N. Sfina [a], N. Bouarissa [b], M. Said [a]

[a] Unité de Recherche de Physique des Solides, Département de Physique, Faculté des Sciences de Monastir, 5019 Monastir, Tunisia
[b] Department of Physics, Faculty of Science, King Khalid University, Abha, PO Box 9004, Saudi Arabia

ARTICLE INFO

Article history:
Received 4 January 2011
Received in revised form 9 May 2011
Accepted 10 May 2011
Available online 18 May 2011

Keywords:
II–VI semiconductors
Band offset calculation
Magnetic effect in DMSs
sp–d exchange interaction
Ternary alloys

ABSTRACT

Due to the large variety of properties offered by the telluride binaries CdTe, ZnTe, MgTe, HgTe and MnTe as well as their mixed ternary alloys, an accurate knowledge of their electronic band parameters is crucial. These materials have been extensively studied but, some points bearing on several properties have never previously reported or are still not clear. In this paper, we report results on the conduction and valence band offsets of the pseudo-morphically strained $Cd_{1-x}X_xTe$ layer on relaxed $Cd_{1-y}X_yTe$ substrate, X = Zn, Hg, Mg and Mn. Based on the Van Der Walle model, calculations have been performed for the all range of material and substrate $0 \le x,y \le 1$. These discontinuities have not yet calculated for X = Mg, Mn or Hg in the all range $0 \le x,y \le 1$. For the CdMnTe diluted magnetic semiconductor which we focus more interest due to its considerable current interest for applications, calculations have been done without and with correction taking into account magnetic effect of magnesium ions Mn^{2+}. It is found that the introduction of only a few percent of Mn into CdTe provides a unique opportunity to combine two important fields in physics, semiconductivity and magnetism. We can take advantage both of possibility of applications in solid-state lasers and exceptional magnetic properties offered by this magnetic diluted semiconductor.

This study presents important quantities that are required to model quantum structures and offers a fast and inexpensive way to check device designs and processes.

1. Introduction

Due to the necessity for optoelectronic devices incessantly increasing, scientists' efforts must be multiplied and progress in growth techniques must be done. Recently, there has been a renewed interest in heterostructures made of II–VI compounds, a group of semiconductors that covers a broad range of energy gaps and lattice constants. Because of the large variety of properties offered by these materials, the focus of interest can be divided into three areas: (i) the wide gap semiconductors, illustrated by the Zn-compounds, are attractive for light-emitting, display and, more recently, possible optical storage applications, (ii) the Hg-compounds with energies in the infrared domain always are important as detectors and imaging devices in this spectral range, (iii) another class, no less important consists of materials which form solid solutions with magnetic elements, known as the diluted magnetic semiconductors (DMSs). The most commonly studied among these is the CdMnTe. The real interest in DMSs, however, lies in providing a unique opportunity to combine two important fields in physics, semiconductivity and magnetism [1].

In fact, CdTe and its ternary alloy $Cd_{1-x}Zn_xTe$ are important semiconductor materials used in solar cells, X-ray detectors and other optoelectronic devices [2–4]. CdMgTe used in solar cells offers a largest range of energy gaps with the least addition of Mg. However, $Cd_xHg_{1-x}Te$, with its band gap varying from 0 semi metal HgTe to semiconductor CdTe, is an extensively used material for emission in the mid-infrared (MIR) spectral domain. CdTe and HgTe compounds interdiffuse easily [5,6] and the solid solution $Cd_{1-x}Hg_xTe$ exists for values of x ranging from 0 to 1 so that any energy band gap from 0 to 1.6 eV is obtained by a sample thermal treatment [7]. On the other hand, $Cd_{1-x}Mn_xTe$ is a diluted magnetic semiconductor with zinc blende structure for $x < 0.77$ [8] which has been of great importance in experimental and theoretical works during the last few decades and has emerged as great promising candidate in wide fields of applications [9–12]. $Cd_{1-x}Mn_xTe$ crystal possesses the applications in a number of devices not only owing to its unique magnetic and magneto-optic properties discovered and investigated [13,14], but also because of some unique properties leading to its potential use in a wide range of optoelectronic applications. In fact, $Cd_{1-x}Mn_xTe$ crystals can be used as substrates for the epitaxial growth due to the variable lattice constant as a function of the Mn content to match the lattice of the epitaxy layer [15]. Moreover, $Cd_{1-x}Mn_xTe$ is demonstrated to be a good candidate to compete with $Cd_{1-x}Zn_xTe$ in the X-ray detector application,

* Corresponding author. Tel.: +216 7350 0274; fax: +216 7350 0278.
E-mail address: samiaabdi@myway.com (S. Abdi-Ben Nasrallah).

0925-8388/$ – see front matter © 2011 Elsevier B.V. All rights reserved.
doi:10.1016/j.jallcom.2011.05.036

because Mn distributes more homogeneously than Zn and that is an excellent alternative for room temperature mid-infrared photonic devices [16,17]. II–VI semiconductors form a unique system where Mn is an isoelectronic magnetic impurity, so that carrier density can be controlled independently of magnetic ion concentration. In particular, modulation doping can be used to introduce a 2D electron or hole gas in a quantum well containing a diluted magnetic semiconductor. However, despite intensive research on this compound and the remarkable progress in device performance, the values of the conduction and valence band offsets are either unknown or usually approximated by their values in the binary alloy and understanding of its optical and structural properties is still not satisfactory.

For those entire requests and in the aim to determine parameters indispensable in the modelling of designs based on $Cd_{1-x}X_xTe$, we suggest the Van Der Walle model to determine the valence and conduction band offsets (BO) of strained $Cd_{1-x}X_xTe$ on relaxed $Cd_{1-y}X_yTe$ for the entire range $0 \le x \le 1$. In the case of $Cd_{1-x}Mn_xTe$, the magnetic field effect on band discontinuities is taken into account.

The paper is arranged as follows. After a brief introduction, we present theoretical model used in the band offsets investigations in Section 2. Results of calculation are discussed and compared with available experimental results in Section 3 for $Cd_{1-x}X_xTe/Cd_{1-y}X_yTe$ interfaces, X = Zn, Mg, Hg and Mn. In the case of $Cd_{1-x}Mn_xTe/Cd_{1-y}Mn_yTe$, our calculations deal both without and with taking into account the magnetic effects. The conclusion is given in Section 4.

2. Methods of calculation

2.1. Strain equations

The lattice mismatch between SCs can be accommodated by lattice strains in sufficiently thin layers which can cause profound changes in the electronic properties and therefore provide extra flexibility in device design. The knowledge of the discontinuities in valence and conduction bands at SC interfaces is essential for the analysis of the properties of any hetero-junction. However, despite intensive research on $Cd_{1-x}X_xTe$ compounds X = Zn, Mg, Hg and Mn, to the best of our knowledge, band offset calculations have never previously reported for the entire range $0 \le x \le 1$ semiconductor ternary alloys. The values of the conduction and valence band offsets (CBOs and VBOs) are either unknown or usually approximated by their values in the binary alloy. To evaluate these band offsets, the model-solid theory of Van Der Walle and Martin [18] is practical and can be used for lattice-matched and lattice-mismatched interfaces. This model is based on the definition of a reference energy for valence band $E_{v,av}$ defined as the average over the uppermost valence bands at the point of the Brillouin zone. We consider that, under pseudomorphic conditions, strains are sufficiently small to be in the linear regime and the strain direction is the z-axis direction of growth. The band energy shifts are related to strains by making use of deformation potentials. The calculations of the offsets at $Cd_{1-x}X_xTe/Cd_{1-y}X_yTe$ interface with $0 \le x,y \le 1$ are assessed as described in our previous work [19]. The CdX and XTe semiconductors have the zinc blende structure with a band structure that includes three degenerate valence bands at Γ. These bands, labelled here by $E_{v,hh}$, $E_{v,lh}$ (the heavy and light hole bands) and $E_{v,so}$ (the split-off band), are strictly degenerate only in the absence of strain and spin–orbit splitting. When no strain is present, spin–orbit interaction splits the valence bands into heavy and light hole bands and the spin–orbit band, the corresponding energy is denoted as Δ_0. The hydrostatic component of the strain shifts the bulk energy levels of layers, and the shear component causes splitting of certain degenerate valence band levels, which interact with spin–orbit splitting to produce the final valence band positions.

The strains splitting themselves are proportional to the magnitude of strain and are described in terms of the deformation potentials. For strain along [0 0 1] direction of $Cd_{1-x}X_xTe/Cd_{1-y}X_yTe$ heterostructure, the shifts of the valence and conduction bands are given by:

$$\begin{aligned}\delta E_{v,hh}(x,y) &= a_v(x)(2\varepsilon_{II}+\varepsilon_\perp) - 0.5\delta E_{0\,0\,1}\\ \delta E_{v,hh}(x,y) &= 2a_v(x)\varepsilon_{II}\left(1-\frac{C_{12}(x)}{C_{11}(x)}\right) - 0.5\delta E_{0\,0\,1}\end{aligned} \tag{1}$$

$$\begin{aligned}\delta E_{v,lh}(x,y) = {} & 2a_v(x)\varepsilon_{II}\left(1-\frac{C_{12}(x)}{C_{11}(x)}\right) - \frac{\Delta_0(x)}{2} + 0.25\delta E_{0\,0\,1}\\ & + 0.5\left[\Delta_0^2(x) + \Delta_0(x)\delta E_{0\,0\,1} + 2.25(\delta E_{0\,0\,1})^2\right]^{1/2}\end{aligned} \tag{2}$$

$$\begin{aligned}\delta E_{v,so}(x,y) = {} & 2a_v(x)\varepsilon_{II}(1-\frac{C_{12}(x)}{C_{11}(x)}) + \frac{\Delta_0(x)}{2} + 0.25\delta E_{0\,0\,1}\\ & - 0.5\left[\Delta_0^2(x) + \Delta_0(x)\delta E_{0\,0\,1} + 2.25(\delta E_{0\,0\,1})^2\right]^{1/2}\end{aligned} \tag{3}$$

$$\begin{aligned}\delta E_c(x,y) &= a_c(x)(2\varepsilon_{II}+\varepsilon_\perp)\\ \delta E_c(x,y) &= 2a_c(x)\varepsilon_{II}\left(1-\frac{C_{12}(x)}{C_{11}(x)}\right)\end{aligned} \tag{4}$$

In these equations, $\delta E_{0\,0\,1}$ is given by:

$$\begin{aligned}\delta E_{0\,0\,1} &= 2b(x)(\varepsilon_\perp - \varepsilon_{II})\\ \delta E_{0\,0\,1} &= -2b(x)\varepsilon_{II}\left(2\frac{C_{12}(x)}{C_{11}(x)}+1\right)\end{aligned} \tag{5}$$

The components of the strain tensor for $Cd_{1-x}X_xTe$, $\varepsilon_{xx} = \varepsilon_{yy} = \varepsilon_{II}$ and $\varepsilon_{zz} = \varepsilon_\perp$ are given by:

$$\varepsilon_{II} = \frac{a_{II}}{a} - 1 = \frac{a(y)}{a(x)} - 1 \tag{6}$$

$$\varepsilon_\perp = \frac{a_\perp}{a} - 1 = -2\frac{C_{12}(x)}{C_{11}(x)}\varepsilon_{II} \tag{7}$$

with a_{II} and a the substrate and the unstrained over-layer lattice constants while $a_\perp$ is the perpendicular over-layer lattice constant given, in the [0 0 1] direction, by $a_\perp = a\left\{1 - 2(C_{12}(x)/C_{11}(x))((a_{II}/a)-1)\right\}$.

The subscript $\perp$ designs the direction perpendicular to the interface between substrate and over layer. b is the shear deformation potential for the valence band, a_c and a_v are the hydrostatic deformation potential for the conduction and the valence bands respectively, and C_{ij} designate the elastic coefficients for the material under consideration.

Thus, the valence and conduction band offsets including strain effects for the $Cd_{1-x}X_xTe/Cd_{1-y}X_yTe$ heterojunction are:

$$\Delta E_{v,hh,lh,so}(x,y) = \Delta E_v^{unst}(x,y) + \delta E_{v,hh,lh,so}(x,y) \tag{8}$$

$$\Delta E_c(x,y) = \Delta E_v^{unst}(x,y) + \Delta E_g^{unst}(x,y) + \delta E_c(x,y) \tag{9}$$

where ΔE_v^{unst} represents the difference between valence band energies between $Cd_{1-x}X_xTe$ and $Cd_{1-y}X_yTe$ unstrained materials, ΔE_g^{unst} denotes the band gap differences, $\delta E_{v,hh,lh,so}$ and δE_c are the valence and conduction band offset shifts due to the strain.

$$\delta E_{v,hh,lh,so}(x,y) = \delta E_v^{hyd}(x,y) + \delta E_{v,hh,lh,so}^{shear}(x,y) \tag{10}$$

The first term in the valence band shift is the hydrostatic correction and the second is the shear one. While our ternaries have direct gap along the x composition range, for the conduction band, solely the hydrostatic strain acts and generates the following shift:

$$\delta E_c(x,y) = \delta E_c^{hyd}(x,y) \tag{11}$$

2.2. Effect of magnetic field on band offsets

However, while CdMnTe is a DMS, we must take into account the magnetic effect introduced by Mn atoms. One of the most spectacular phenomenons in DMS is enhancement of Zeeman splitting, called giant Zeeman effect, as a result of a strong interaction between the magnetic ions and carriers [20,21]. In fact, the polarisation of the localized magnetic spins leads to an effective magnetic field felt by spin carriers. The enhancement is due to exchange interaction between localized Mn spins and delocalized carriers of valence and conduction bands. In the mean-field approximation inserting the mean value of Mn spin when magnetic field oriented along z axis, the hamiltonian operator of exchange interaction can be written in simplified form [21]:

$$H_{s-d} = N_0\alpha x_{Mn}\langle S_z\rangle\sigma \tag{12}$$

for the conduction electrons and:

$$H_{p-d} = \frac{1}{3}N_0\beta x_{Mn}\langle S_z\rangle J \tag{13}$$

for valence band holes. σ and J denote the electron spin ($\pm 1/2$) and the total angular momentum of the hole ($\pm 3/2$ for heavy holes and $\pm 1/2$ for light holes) respectively. x_{Mn} is the effective Mn concentration in $Cd_{1-x}Mn_xTe$ given by the expression $x_{Mn}(x) = (2/5)(x/1100)\left[718.2\exp(-(x/0.02307)) + 1988(-(x/0.01615)) + 19.66\right]$ [22], N_0 is the number of crystalline elementary cells per unit volume, α (β) are values of s–d (p–d) exchange integrals. Values of the parameters determined experimentally by Gaj et al. [20] for (Cd,Mn)Te are $N_0\alpha = 0.220$ eV and $N_0\beta = -0.880$ eV. $\langle S_z\rangle$ is the thermodynamic average value of Mn spin along z axis given by:

$$\langle S_z\rangle = SB_S\left\{\frac{g_{Mn}\mu_B BS}{k_B(T+T_0)}\right\} \tag{14}$$

Table 1
Parameters of binaries used in band offset calculations: lattice parameter a, band gap energy, spin–orbit splitting Δ_0, the average energy of the three uppermost valence bands $E_{v,av}$, experimental values of hydrostatic deformation potential for the valence and conduction bands a_v and a_c, experimental uniaxial deformation potential b.

	CdTe	ZnTe	MnTe	MgTe	HgTe
C_{11} (10^{10} N/m^2)	5.35 [24]	7.13 [24]	4.74 [24]	6.124 [2]	5.361 [1]
C_{12} (10^{10} N/m^2)	3.68 [24]	4.07 [24]	3.29 [24]	2.817 [2]	3.66 [18]
a (Å)	6.481	6.103	6.338	6.35	6.461
E_g (eV)	1.606	2.39	3.198	3.6	0
Δso_{exp}	0.9 [25]	0.9 [25]	0.42	0.945	0.9 [25]
(eV)	0.85 [23]	0.8 [23]	[23]	[2]	0.8 [18]
a_c (eV)	−2.15 [26]	−3.5 [26]	–	−3 [29]	−4.60 [18]
a_v	1.18 [26]	1.8 [26]	–	1.58	−0.13
(eV)	−1.28 [27]	−1.82 [27]		[29]	[18]
	0.5 [18]	0.8 [18]			
b	−1.4 [26]	−0.92 [26]	–	–	−1.15
(eV)	−1.10 [18]	−1.26 [18]			[18]
	−1.15 [27]	−1.3 [27]			
E_c (eV)	−5.17 [18]	−4.48 [18]	–	–	−6.83 [18]
$E_{v,av}$	−7.07 [18]	−7.17 [18]	–	–	−6.88 [18]
(eV)	−6.62 [28]	−6.74 [28]			−6.38 [28]

All these parameters are given in eV. The elastic constants C_{11} and C_{12} are in 10^{10} N/m^2.

where S is the effective spin of Mn ion equal to 5/2, B_S is the Brillouin function, g_{Mn} is the Mn Lande factor, equal to 2, μ_B is the Bohr magneton, k_β is the Boltzmann constant. T_0 is a phenomenological parameter introduced for adjusting the effective temperature further to antiferromagnetic interaction. This adjustment was found to depend on Mn composition x [22] as follows:

$$T_0(x) = \frac{35.37x}{1 + 2.752x}, \quad (\text{in K}) \tag{15}$$

We note that we discuss only the giant Zeeman effect. In fact, for low values of magnetic field, less than 5 T, the Zeeman effect and Landau quantification can be neglected.

Then, the conduction band offsets, heavy hole and light hole band offsets in the presence of magnetic fold B can be deduced by:

$$\Delta E_{c,\pm 1/2}(B,x) = \Delta E_c(B=0) \pm \frac{1}{2} N_0 \alpha x_{Mn} \langle S_z \rangle \tag{16}$$

$$\Delta E_{v,\mathrm{hh},\pm 3/2}(B,x) = \Delta E_{v,\mathrm{hh}}(B=0) \pm \frac{1}{2} N_0 \beta x_{Mn} \langle S_z \rangle \tag{17}$$

$$\Delta E_{v,\mathrm{lh},\pm 1/2}(B,x) = \Delta E_{v,\mathrm{lh}}(B=0) \pm \frac{1}{6} N_0 \beta x_{Mn} \langle S_z \rangle \tag{18}$$

where $\Delta E_c(B=0)$, $\Delta E_{v,\mathrm{hh}}(B=0)$, and $\Delta E_{v,\mathrm{lh}}(B=0)$ are the conduction, heavy hole and light hole band offsets respectively under zero magnetic field. Second terms in Eqs. (16)–(18) are the corrections introduced by the magnetic effect on conduction and valence bands describing the splitting.

3. Results and discussion

Due to the fact that the values of the CBOs and VBOs are crucial in the modelling of designs, we present now our results for BOs of strained $Cd_{1-x}X_xTe$ on relaxed $Cd_{1-y}X_yTe$ with $0 \le x,y \le 1$. Our procedure has been to use calculated valence-band positions and add the reported band gap to obtain conduction-band positions. In Table 1, are given the parameters used in band offset calculation for binaries CdTe, ZnTe, HgTe, MgTe and MnTe, those of ternary alloys are estimated from a linear interpolation. However, there are some missing values in Table 1. In fact, unlike CdTe, ZnTe and HgTe which have been extensively studied, very little about MnTe and MgTe. In Ref. [30], the authors have taken the valence-band parameters of MgTe to be similar to these of CdTe. The parameters of $Cd_{1-x}Mg_xTe$ alloys are obtained by a linear interpolation between the corresponding CdTe and MgTe data. In Ref. [29], the authors have extracted the hydrostatic deformation potential for the conduction and the valence bands respectively, a_c and a_v for MgTe as well as the discontinuities at the interface of binaries CdTe/MgTe. This latter allows deducing the E_v corresponding to MgTe. For MnTe binary, we have also used the same parameters.

We mention that, we have taken for ternary alloys the gap expressions available in the literature taking into account the disorder effect [8,31,32].

We would point out that for the II–VI heterostructures, the Coulombic interactions are important given rise to the exciton formation, and affecting the potential profiles. In studying the tunneling dynamics in CdTe/(Cd,Zn)Te asymmetric double-quantum-well structures, Haacke et al. [33] showed that for the tunneling mechanism, it is identified the importance of excitons rather than free-carrier states. On the other hand, optical experiments on excitonic effects in separate-confinement quantum-well heterostructures CdTe/(Cd,Zn)Te were performed by Deleporte et al. [34] who showed that due to the Coulombic interaction between the localized electrons and the light holes, the potential offsets are completely changed from type-II (due to the strains) to type-I behaviour of the 1s light-hole excitonic recombination line. As far as the heterostructures are concerned, in the present investigation the values of all band offsets of interest are found to be larger than the excitonic effect. Hence, in our analysis this effect was not taken into consideration.

3.1. CdZnTe

Results of BO calculation are illustrated in Fig. 1(a–c) as a function of Zn compositions x and y in the material and in the substrate respectively. Due to the lower lattice parameter of ZnTe than the one of CdTe, for the case of $x < y$, the substrate lattice parameter is smaller than the material one and the epitaxial layer is under compressive strain. In view of Fig. 1, one can note that the band offsets are small in the valence band (from −0.200 to 0.240 eV for heavy hole and from −0.040 to 0.200 eV for light hole). We should also mention that under compressive biaxial strain (growth on a substrate with smaller lattice constant $x < y$), the heavy hole band will be at the band edge ($\delta E_{v,\mathrm{hh}} > \delta E_{v,\mathrm{lh}}$). For heavy holes, the iso-energy band offsets are practically linear whereas a non-linear behaviour characterizes the conduction band offsets and the light hole ones especially in the compressive strain case. For $Cd_{1-x}Zn_xTe/Cd_{1-y}Zn_yTe$ with $x = 0$, i.e. for $CdTe/Cd_{1-y}Zn_yTe$ interface, the band lineup is of type I for e–hh transition and of type II for e–lh transition, this result is in agreement with Mariette et al. [35]. In the case of CdTe/ZnTe interface, our values are as good as with those reported in the literature. We found $\Delta E_c = 0.570$, $\Delta E_{hh} = 0.250$ and $\Delta E_{lh} = 0.028$ eV while Oh et al. [36] found 0.696, 0.2 and 0.11 eV for CBO, heavy hole BO and light hole BO respectively. We can also notice that under compressive biaxial strain (growth on a substrate with smaller lattice constant $x < y$), for the same value of Zn content in the material $x = 0.21$, the same light hole band offset (Fig. 1c) is obtained with different values of Zn content in the substrate y. The lower value of y is the more interesting because it is the near of the

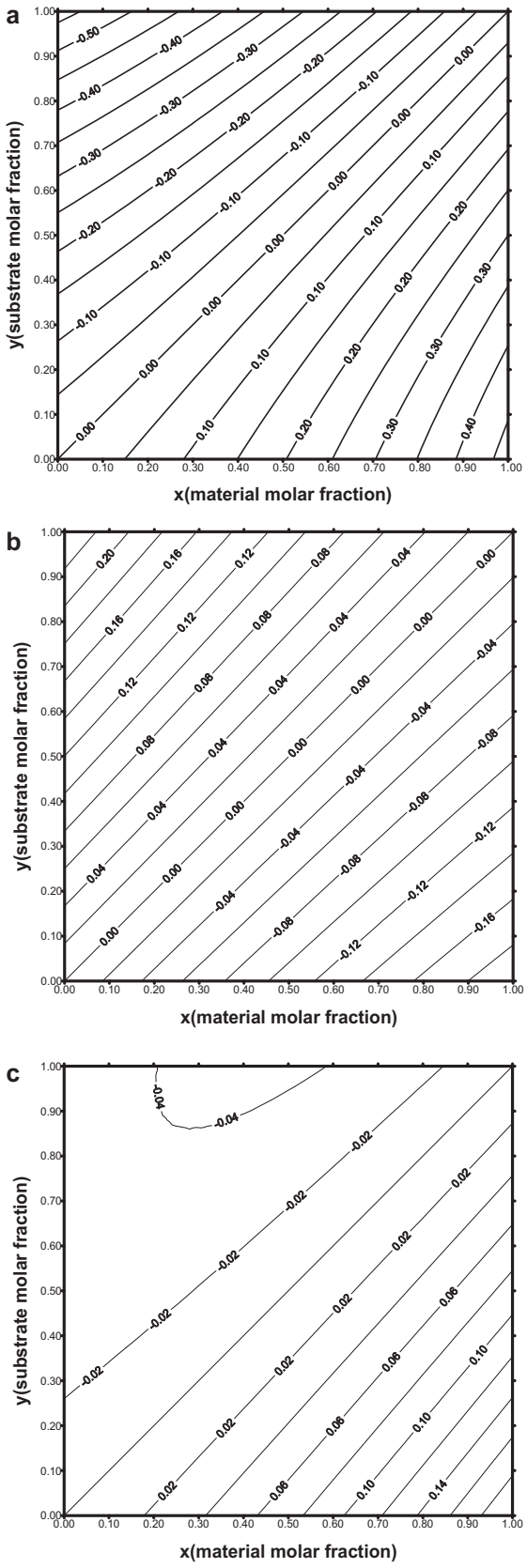

Fig. 1. Conduction band offset ΔE_c (a), valence band offsets for heavy hole $\Delta E_{v,\mathrm{hh}}$ (b) and for light hole $\Delta E_{v,\mathrm{lh}}$ (c) in (0 0 1) $Cd_{1-x}Zn_xTe/Cd_{1-y}Zn_yTe$ interface. All band offsets are given in eV.

condition of lattice matching $\Delta a/a = 0$. From Fig. 1(a and b) one can also remark that for $x > y$ and $x < y$, the conduction BO ΔE_c and the heavy hole valence BO ΔE_{hh} have opposite signs, so, the line-up of $e \rightarrow$ hh transition is of type I in the all range $0 \leq x, y \leq 1$.

3.2. CdMgTe

Concerning the $Cd_{1-x}Mg_xTe/Cd_{1-y}Mg_yTe$ interface our band offsets are depicted in Fig. 2(a–c) as a function of Mg contents x and y in the material and in the substrate respectively. Due to the lower lattice parameter of MgTe than the one of CdTe, for the case of $x < y$, the substrate lattice parameter is smaller than the material one and the epitaxial layer is under compressive strain. The band offsets are large in the conduction band (from −1 to 1 eV for $0 \leq x,y \leq 1$), a little smaller in the valence bands (from −0.750 to 0.750 eV for heavy hole and from −0.610 to 0.630 eV for light hole). The iso-energy band offsets are practically linear. However, even if the band-offset variations are linear, we think these abacuses useful to the scientific community to determine the band diagram of the considered heterostructures for all alloy compositions in material and substrate. The heavy hole valence band offsets increase (decrease) when material $Cd_{1-x}Mn_xTe$ is under compressive (tensile) strain. As seen in Fig. 2, it is found that the conduction and heavy hole band offsets have opposite signs in the compressive or tensile strain, so, the line-up is of type I. We note that our calculated valence band offsets for CdTe/MgTe (0.75 eV), $CdTe/Cd_{0.65}Mg_{0.35}Te$ (0.26 eV) agree with those given in Refs. [37] and [38] respectively. Note that this later is given for $Cd_{0.95}Mn_{0.05}Te/Cd_{0.65}Mg_{0.35}Te$ interface. In the case of $CdTe/Cd_{0.9}Mg_{0.1}Te$, we found $\Delta E_v = 0.075$ eV and $\Delta E_c = 0.065$ eV while Kowalczky et al. have given the values 0.043 eV and 0.10 eV in their Ref. [39].

3.3. CdHgTe

Our calculated band offsets for $Cd_{1-x}Hg_xTe/Cd_{1-y}Hg_yTe$ interface are plotted in Fig. 3(a–c) as a function of Hg contents x and y in the material and in the substrate respectively. The band offsets are large in the conduction band (from −1.800 to 1.800 eV for $0 \leq x,y \leq 1$), but small in the valence band (from −0.225 to 0.225 eV for heavy hole and from −0.250 to 0.250 eV for light hole). For heavy and light holes, the iso-energy band offsets are practically linear whereas a nonlinear behaviour characterizes the conduction band offset. The same value of CBO corresponding to Hg content in the material (x) can be achieved with two different y values of substrate Hg content. This anomaly has been shown also in lh valence band offset of $Cd_{1-x}Zn_xTe/Cd_{1-y}Zn_yTe$ interface. Fig. 3(a and b) shows that (i) for $x > y$, the line-up is of type I when y is lower than 0.48 and of type II when y is higher than 0.48; (ii) for $x < y$, the line-up is of type I when x is lower than 0.48 and of type II when x is higher than 0.48. For CdTe/HgTe, the debate about the valence band-offset for HgTe–CdTe superlattice was even between values going from 30 meV to 800 meV. In fact, early magneto-optical measurements give very small valence band discontinuities from 0 to 0.063 eV [40–42]. Later magneto-optical measurements give very high values 0.55–0.80 eV [43,44]. Experimental results are more consistent with moderate values of 0.35–0.39 eV [39,45,46] and theoretical calculations have been carried out to resolve this controversy with values of band discontinuity in favor of later experimental values [47,48]. Ekpunobi [49] has used a tight binding method to calculate the valence band discontinuity at the $CdTe/Hg_xCd_{1-x}Te$ interface. The calculated valence band offset of 0.31 eV at CdTe/HgTe interface which is close to the self-consistent calculations of 0.30 eV [50] and in good agreement with experimental values of 0.35 eV [39,51]. Calculations were extended to alloy interfaces.

Our result for the VBO at CdTe/HgTe interface ($x = 0$ and $y = 1$) $\Delta E_{\mathrm{hh}} = 0.223$ eV are in good agreement with the value 0.23 eV

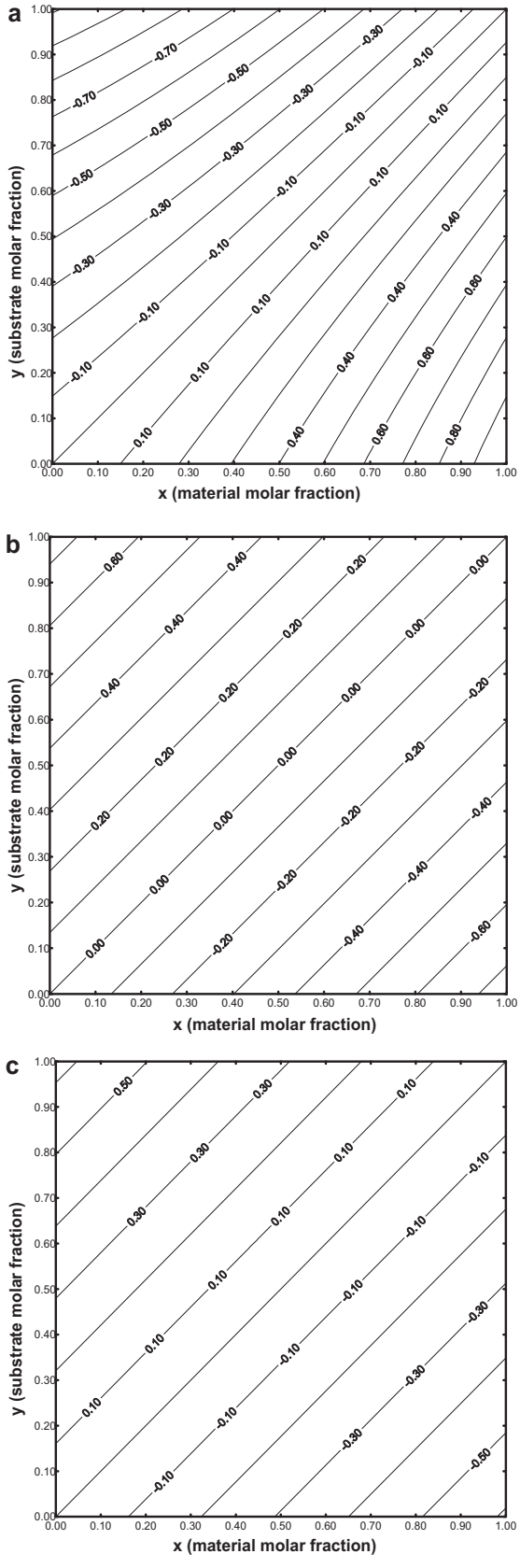

Fig. 2. Conduction band offset ΔE_c (a), valence band offsets for heavy hole $\Delta E_{v,\mathrm{hh}}$ (b) and for light hole $\Delta E_{v,\mathrm{lh}}$ (c) in (0 0 1) $Cd_{1-x}Mg_xTe/Cd_{1-y}Mg_yTe$ interface.

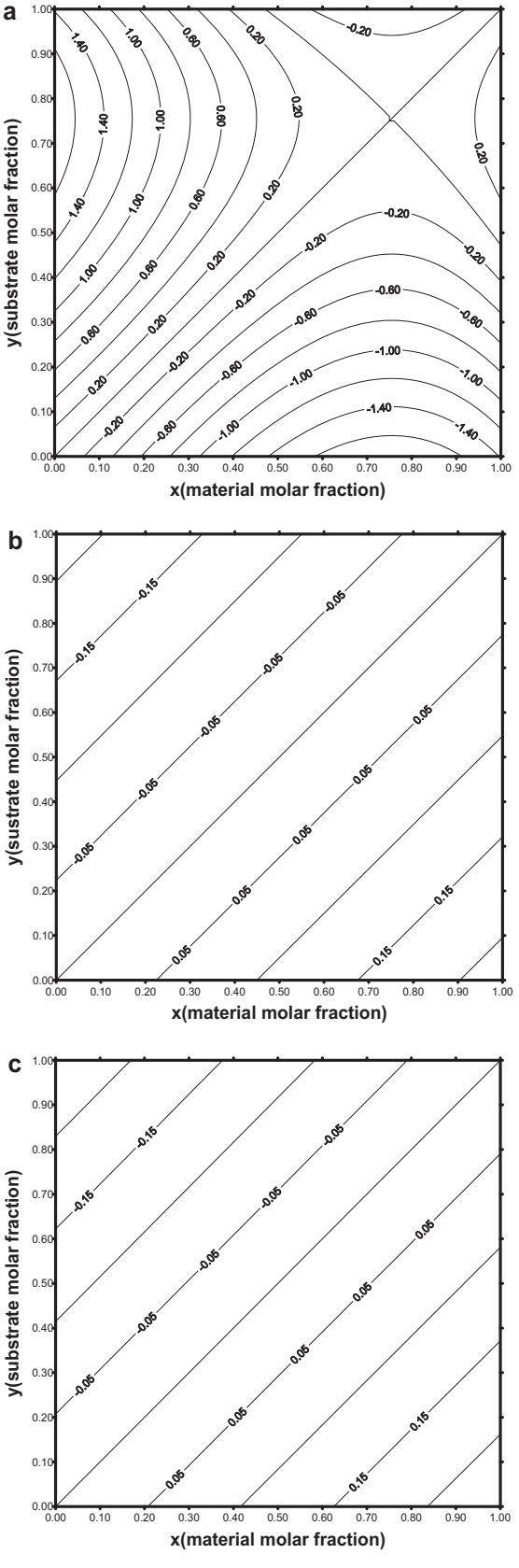

Fig. 3. Conduction band offset ΔE_c (a), valence band offsets for heavy hole $\Delta E_{v,\mathrm{hh}}$ (b) and for light hole $\Delta E_{v,\mathrm{lh}}$ (c) in (0 0 1) $Cd_{1-x}Hg_xTe/Cd_{1-y}Hg_yTe$ interface.

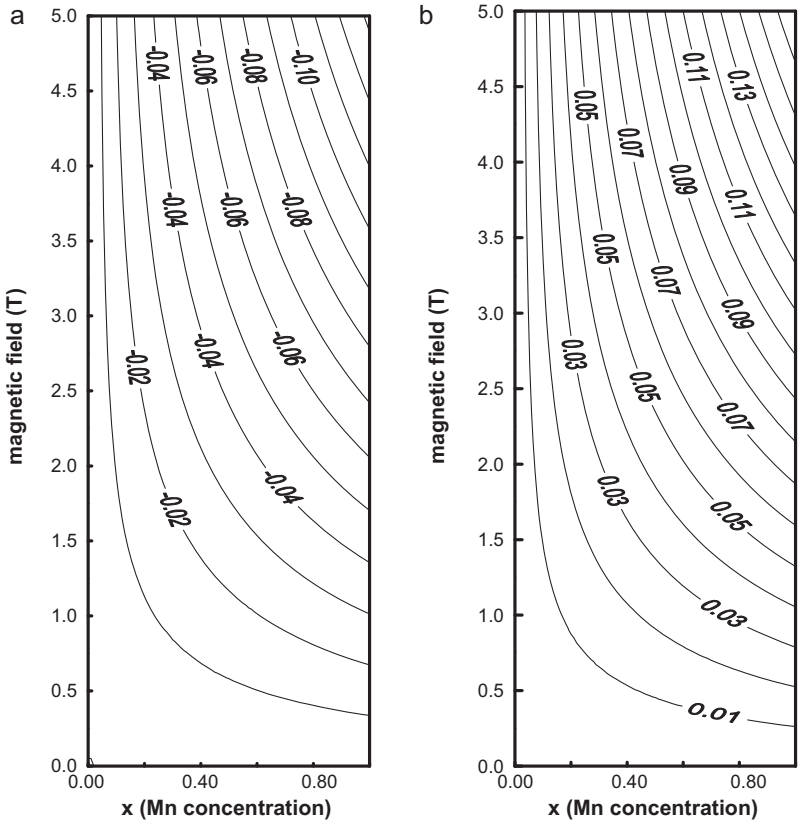

Fig. 4. Correction induced by magnetic field effect on conduction (a) and valence (b) bands of $Cd_{1-x}Mn_xTe$ for $0 \leq x \leq 1$ Mn content.

reported in Ref. [18] and agree reasonably with the value 0.3 given in Ref. [50] and the value 0.36 ± 0.06 eV reported in Ref. [39]. For conduction band offset, we found 1.380 eV while authors of Ref. [49] found 1.590 eV.

3.4. CdMnTe

The CdMnTe semimagnetic semiconductor and related nanostructures belong to attractive materials owing to their unique properties and because of new possibilities of application in spintronic devices. Our band offsets calculated for $Cd_{1-x}Mn_xTe/Cd_{1-y}Mn_yTe$ interface, without taking into account the magnetic effects, are identical to $Cd_{1-x}Mg_xTe/Cd_{1-y}Mg_yTe$ interface (Fig. 2(a–c)) due the same parameters used in the calculation. While the magnetic interaction between carrier moments and those of Mn atoms is inevitable, the correction induced on conduction and valence band offsets given by Eqs. (12) and (13) are illustrated in Fig. 4(a and b) respectively as a function of Mn content x and magnetic field B. The band offsets change drastically in the presence of a magnetic field. The strong sp–d exchange interaction between carriers and Mn spins gives rise to a large splitting which can attain 100 meV for high Mn content values. Our predictions for shift in CBO of 0.169 eV for electrons and in VBO of 0.074 eV for heavy holes in $CdTe/Cd_{0.8}Mn_{0.2}Te$ interface at 0.1 T agree very well with Adachi et al. calculation [38] who found 0.176 and 0.075 eV respectively. Christensen et al. [52] give a value of VBO between 0.7 and 0.8 eV for CdTe/MnTe interface.

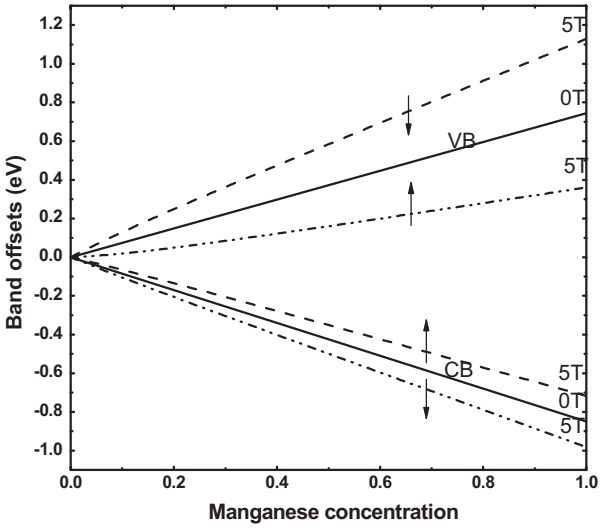

Fig. 5. Conduction and heavy hole valence band offsets of $Cd_{1-x}Mn_xTe/CdTe$ interface versus manganese composition x for magnetic field values of 0 and 5 T.

Then, we have illustrated the splitting of the conduction and heavy hole valence band offsets in Fig. 5 for $Cd_{1-x}Mn_xTe/CdTe$ interface in the whole range of Mn composition x and for magnetic field values equal to 0 and 5 T. The splitting for the two possible orientations of spin, $\pm 1/2$ for electrons and $\pm 3/2$ for heavy holes are given for x ranging from 0 to 1.

4. Conclusions

Several studies have been done on the ternary cubic $Cd_{1-x}X_xTe$, X = Zn, Mg, Hg and Mn but to our knowledge, the compositional dependence band discontinuities have not been performed until now for the all range of material and substrate compositions. This paper is devoted to calculate these band offsets and assess more carefully the effect of magnetic Mn ions on band offsets of $Cd_{1-x}Mn_xTe$ alloys. The conduction and valence band offsets of

the relaxed and pseudomorphically strained $Cd_{1-x}X_xTe/Cd_{1-y}X_yTe$ interface are performed using the Van der Walle model-solid theory. In the case of CdMnTe, the strong exchange interaction between the local moments of the magnetic ions and the spins of band holes gives rise to a dramatic enhancement of the Zeeman splitting. The magnetic substitution makes it possible to tune with both the composition and the magnetic field many of the electronic and magnetic properties, leading to a variety of device possibilities.

The information derived from the present study demonstrates the potential of the materials of interest for optoelectronic, photovoltaic and spintronic device applications.

References

[1] L.L. Chang, Superlattices Microstruct. 6 (1989) 39.
[2] R.K. Willardson, A.C. Beer, Semiconductors and Semimetals, vol. 13, Academic Press, New York, 1978.
[3] T.E. Schlesinger, R.B. James, Semiconductors and Semimetals, vol. 43, Academic, San Diego, 1995.
[4] Z.Q. Shi, C.M. Stahle, P. Shu, Proc. SPIE 3553 (1998) 90.
[5] G. Cohen-Solal, Y. Marfaing, F. Bailli, Rev. Phys. Appl. 1 (1966) 11.
[6] R. Triboulet, Rev. Phys. Appl. 2 (1977) 123.
[7] A. Bouazzi, Y. Marfaing, J. Mimila Arroyo, Rev. Phys. Appl. 13 (1978) 145.
[8] J.K. Furdyna, J. Appl. Phys. R 29 (1988) 64.
[9] W. Grieshaber, A. Haury, J. Cibert, Y. Merle D'Aubigné, A. Wasiela, Phys. Rev. B 53 (1996) 4891.
[10] V.V. Fedorov, W. Mallory, S.B. Mirov, U. Hömmerich, S.B. Trivedi, W. Palosz, J. Cryst. Growth 310 (2008) 4438.
[11] L.-C. Tung, G. Karczewski, Y.J. Wang, Physica E 40 (2008) 1608.
[12] J. Zhang, W. Jie, T. Wang, D. Zeng, S. Ma, H. Hua, B. Yang, Mater. Res. Bull. (2008) 1239.
[13] R.R. Galazka, S. Nagata, P.H. Keesom, Phys. Rev. B 22 (1980) 3344.
[14] D.U. Bartholomew, J.K. Furdyna, A.K. Ramdas, Phys. Rev. B 34 (1986) 6943.
[15] R. Triboulet, A. Heurtel, J. Rioux, J. Cryst. Growth 101 (1990) 131.
[16] A. Mycielski, A. Burger, M. Sowinska, M. Groza, A. Szadkowski, P. Wojnar, B. Witkowska, W. Kaliszek, P. Siffert, Phys. Status Solidi C 5 (2005) 1578.
[17] S.B. Trivedi, C.C. Wang, S. Kutcher, U. Hömmerich, W. Palosz, J. Cryst. Growth 310 (2008) 1099.
[18] C.G. Van de Walle, Phys. Rev. B 39 (1989) 1871.
[19] S. Abdi-Ben Nasrallah, N. Sfina, N. Bouarrissa, M. Said, J. Phys.: Condens. Matter 18 (2006) 3005.
[20] J.A. Gaj, R. Planel, G. Fishman, Solid State Commun. 29 (1979) 435.
[21] J.K. Furdyna, J. Kossut, Semiconductors and Semimetals, (Diluted Magnetic Semiconductors), vol. 25, Academic Press, New York, 1988.
[22] J.A. Gaj, W. Grieshaber, C. Bodin-Deshayes, J. Cibert, G. Feuillet, Y. Merle D'Aubigné, A. Wasiela, Phys. Rev. B 50 (1994) 5512.
[23] S.-H. Wei, A. Zunger, Phys. Rev. B: Condens. Matter 53 (1996) 10457.
[24] L. Börnstein, Numerical Data and Functional Relationships in Science and Technology (Semiconductors), vol. 17, Springer-Verlag, Berlin, 1982.
[25] P. Carrier, S.-H. Wei, Phys. Rev. B 70 (2004) 035212.
[26] H. Mathieu, B. Lefbvre, J. Allegre, J.P. Faurie, Phys. Rev. B 38 (1988) 7740.
[27] P. Peyla, Y. Merle D'Aubigné, A. Wasiela, R. Romestain, H. Mariette, M.D. Sturge, N. Magnea, H. Tuffigo, Phys. Rev. B 46 (1992) 1557.
[28] A. Qteish, R.J. Needs, Phys. Rev. B 45 (1992) 1317.
[29] J.-H. Yang, S. Chen, W.-J. Yin, X.G. Gong, Phys. Rev. B 79 (2009) 245202.
[30] Q.X. Zhao, N. Magnea, J.L. Pautrat, Phys. Rev. B 52 (23) (1995) 16612.
[31] J.M. Hartmann, J. Ciber, F. Kany, H. Mariette, M. Charleux, P. Aleysson, R. Langer, G. Feuillet, J. Appl. Phys. 80 (1996) 6257.
[32] V.A. Tyagai, O.V. Snitko, V.N. Bondarenko, N.I. Vitrikhovskii, V.B. Popov, A.N. Kraziko, Sov. Phys. Solid State 16 (1974) 885.
[33] S. Haacke, N.T. Pelekanos, H. Mariette, M. Zigone, A.P. Heberle, W.W. Rühle, Phys. Rev. B 47 (1993) 16643.
[34] E. Deleporte, J.M. Berroir, C. Delalande, N. Magnea, H. Mariette, J. Allegre, J. Calatayud, Phys. Rev. B 45 (1992) 6305.
[35] H. Mariette, F. Dal'bo, N. Magnea, G. Lentz, H. Tuffigo, Phys. Rev. B 38 (1988) 12443.
[36] S.H. Oh, M.S. Jang, S.H. Kim, J.C. Choi, H.L. Park, D.U. Lee, D.C. Choo, J.H. Kim, M. Jung, T.W. Kim, J. Korean Phys. Soc. 39 (2001) 458.
[37] P. Redliñski, T.G. Rappoport, A. Libal, J.K. Furdyna, B. Jankó, T. Wojtowiczb, Appl. Phys. Lett. 86 (2005) 113103.
[38] S. Adachi, T. Tsuchiya, H. Minoc, S. Takeyama, G. Karczewski, T. Wojitowicz, J. Kossut, Physica E 10 (2001) 305.
[39] S.P. Kowalczyk, J.T. Cheng, E.A. Krout, R.W. Grant, Phys. Rev. Lett. 56 (1986) 1605.
[40] J.M. Berroir, Y. Guldner, J.P. Vieren, M. Voos, J.P. Faurie, Phys. Rev. B 34 (1986) 891.
[41] J. Reno, I.K. Sou, J.P. Faurie, J.M. Berrior, Y. Guldner, J.P. Vieren, Appl. Phys. Lett. 49 (1986) 106.
[42] Z. Yang, J.K. Furdyna, Appl. Phys. Lett. 52 (1988) 498.
[43] M. Von Truchseb, V. Latussek, F. Goschenhofer, C.R. Becker, G. Landwehr, E. Batke, R. Sizmann, P. Helgesen, Phys. Rev. B 51 (1995) 18618.
[44] K.H. Yoo, R.L. Aggarwal, L.R. Ram-Mohan, O.K. Wu, J. Vac. Sci. Technol. A 8 (1990) 1194.
[45] T.M. Duc, C. Hsu, J.P. Faurier, Phys. Rev. Lett. 58 (1987) 1127.
[46] D.H. Chow, J.O. McCaldin, A.R. Bonnefoi, T.C. McGill, I.K. Sou, J.P. Faurie, Appl. Phys. Lett. 51 (1987) 2230.
[47] A. Qteish, R.J. Needs, Phys. Rev. B 47 (1993) 3714.
[48] P.M. Hui, H. Ehrenreich, N.F. Johnson, J. Vac. Sci. Technol. A 7 (1989) 424.
[49] A.J. Ekpunobi, Mater. Sci. Eng. B 117 (2005) 1.
[50] A. Qteish, R.J. Needs, J. Phys.: Condens. Matter 3 (1991) 617.
[51] C.K. Shih, W.E. Spicer, Phys. Rev. Lett. 58 (1987) 2594.
[52] N.E. Christensen, I. Gorczyca, O.B. Christensen, U. Schmid, M. Cardona, J. Cryst. Growth 101 (1990) 318.